

Diffeomorphic demons and the EMPIRE10 challenge

Vincent Garcia¹, Tom Vercauteren²,
Grégoire Malandain¹, and Nicholas Ayache¹

¹ INRIA Sophia Antipolis – Méditerranée, Asclepios Team,
2004 route des lucioles, BP 93, 06902 Sophia Antipolis Cedex, France

² Mauna Kea Technologies, 9 rue d’Enghien, 75010 Paris, France

Abstract. The registration of thoracic images is a common but still challenging problem with critical clinical applications (e.g. radiotherapy and diagnosis). In the context of the EMPIRE10 challenge, we briefly introduce in this paper our registration method based on the diffeomorphic demons algorithm. Although fully automatic and generic (applies to a large variety of images such as brain or thoracic CT scans), the proposed method appears to be a very efficient registration method.

1 Introduction

Registration of thoracic CT images is a challenging problem encountered in the routine clinical life. For instance, one of the most important aspect in radiotherapy planning is to precisely determine the target volume that has to be treated. The elastic nature of the lung tissue deformation and the physiological movement of patient (e.g. breathing cycle) affects the localization of the target volume. Image registration may greatly improve the treatment accuracy by compensating the inevitable anatomical changes between two acquisitions.

Since its publication [?], the *demons* registration algorithm has become a popular and widely used method for intra-modality deformable image registration. Recently, Vercauteren et al. [?] proposed an efficient non-parametric diffeomorphic image registration algorithm based on an extension of the demons algorithm (diffeomorphic demons for short).

EMPIRE10 is a challenge providing a platform for in-depth evaluation and fair comparison of thoracic CT image registration algorithms. In this paper, we apply the diffeomorphic demons registration algorithm in the context of the EMPIRE10 challenge. Although being a generic (can be applied to a large variety of image registration problem) and fully automatic (unique set of parameters), the diffeomorphic demons appears to be a very efficient registration method challenging some other methods highly specialized in the thoracic CT image registration.

2 Diffeomorphic demons

2.1 Standard Demons Algorithm

The demons algorithm alternates between computation of some image warping forces that are inspired by the optical flow and their regularization by a simple Gaussian smoothing. Using a hidden variable in the registration process (correspondences), the demons algorithm can be seen as the optimization of a global energy [?]. The regularization criterion is then considered as a prior on the smoothness of the transformation s . The point correspondences between image pixels (using a vector field c) is not required to be exact realizations of the transformation ; some errors are allowed for each point correspondence. Given a *fixed image* $F(\cdot)$ and a *moving image* $M(\cdot)$, the global energy to be optimized is:

$$E(c, s) = \frac{1}{\sigma_i^2} \text{Sim}(F, M \circ c) + \frac{1}{\sigma_x^2} \text{dist}(s, c)^2 + \frac{1}{\sigma_T^2} \text{Reg}(s) \quad (1)$$

$$\text{Sim}(F, M \circ s) = \frac{1}{2} \|F - M \circ s\|^2 = \frac{1}{2|\Omega_P|} \sum_{p \in \Omega_P} |F(p) - M(s(p))|^2 \quad (2)$$

where Ω_P is the region of overlap between F and $M \circ s$, σ_i accounts for the noise on the image intensity, σ_x accounts for a spatial uncertainty on the correspondences and σ_T controls the amount of regularization we need. We classically have $\text{dist}(s, c) = \|c - s\|$ and $\text{Reg}(s) = \|\nabla s\|^2$ but the regularization can also be modified to handle fluid-like constraints [?]. Within this framework, the demons registration can be explained as an alternate optimization over s and c . It can conveniently be summarized into the algorithm below:

Algorithm 1 Demons algorithm

- 1: Choose a starting spatial transformation (a vector field) s
- 2: **repeat**
- 3: Given s , compute a correspondence update field \mathbf{u} by minimizing

$$E_s^{\text{corr}}(\mathbf{u}) = \|F - M \circ (s + \mathbf{u})\|^2 + \frac{\sigma_i^2}{\sigma_x^2} \|\mathbf{u}\|^2 \quad (3)$$

- 4: with respect to \mathbf{u}
 - 5: **if** a fluid-like regularization is used **then**
 - 6: $\mathbf{u} \leftarrow K_{\text{fluid}} \star \mathbf{u}$.
 - 7: **end if**
 - 8: Let $c \leftarrow s + \mathbf{u}$
 - 9: **if** a diffusion-like regularization is used **then**
 - 10: $s \leftarrow K_{\text{diff}} \star c$.
 - 11: **else**
 - 12: $s \leftarrow c$.
 - 13: **end if**
 - 14: **until** convergence
-

In both steps 5 and 9, the convolution typically uses a Gaussian kernel. Vercauteren et al. [?] showed that a Newton method on $E_s^{\text{corr}}(\mathbf{u})$ explains and generalizes the optimization step advocated by Thirion [?]:

$$\mathbf{u}(p) = -\frac{F(p) - M \circ s(p)}{\|J^p\|^2 + \frac{\sigma_i^2(p)}{\sigma_x^2}} J^{pT} \quad (4)$$

where $\sigma_i(p) = |F(p) - M \circ c(p)|$ is the local estimation of the image noise. $J^p = -\nabla_p^T(M \circ s)$ with a Gauss-Newton method, $J^p = -\frac{1}{2}(\nabla_p^T F + \nabla_p^T(M \circ s))$ with the efficient second-order minimization (ESM) method [?], and $J^p = -\nabla_p^T F$ with Thirion’s rule. Note that σ_x then controls the maximum step length: $\|\mathbf{u}(p)\| \leq \sigma_x/2$.

2.2 Diffeomorphic demons

The most straightforward way to adapt the demons algorithm to make it diffeomorphic is to optimize (1) over a space of diffeomorphisms. This can be done using an intrinsic update step [?,?]

$$s \leftarrow s \circ \exp(\mathbf{u}), \quad (5)$$

on the Lie group of diffeomorphisms. This approach obviously requires an algorithm to compute the exponential for the Lie group of interest. Thanks to the scaling and squaring approach presented in [?], this exponential can efficiently be computed for diffeomorphisms with just a few compositions:

Algorithm 2 Fast computation of vector field exponential

- 1: Choose N such that $2^{-N}\mathbf{u}$ is close enough to 0 (e.g. $\max \|2^{-N}\mathbf{u}(p)\| \leq 0.5$)
 - 2: Perform an explicit first order integration: $v(p) \leftarrow 2^{-N}\mathbf{u}(p)$ for all pixels
 - 3: Do N recursive squarings of v : $v \leftarrow v \circ v$
-

By plugging the above Newton method tools for Lie groups within the alternate optimization framework of the demons, Vercauteren et al. proposed [?] the following non-parametric diffeomorphic image registration algorithm named *diffeomorphic demons*:

Algorithm 3 Diffeomorphic demons iteration

- 1: Compute the correspondence update field \mathbf{u} using (4)
 - 2: If a fluid-like regularization is used, let $\mathbf{u} \leftarrow K_{\text{fluid}} \star \mathbf{u}$.
 - 3: Let $c \leftarrow s \circ \exp(\mathbf{u})$, where $\exp(\mathbf{u})$ is computed using Algorithm 2
 - 4: If a diffusion-like regularization is used, let $s \leftarrow K_{\text{diff}} \star c$ (else let $s \leftarrow c$).
-

3 EMPIRE10 challenge – results

3.1 Challenge context and implementation details

The EMPIRE10 challenge consisted in evaluating the state of the art in chest CT registration. 20 pairs of chest CT scans (intra-subject) had to be registered. The provided data were very challenging since they encompassed many of the problems faced by researchers developing registration algorithms for this application (variation in image/voxel size, scans taken at various phases in the breathing cycle, etc.). In addition to the CT data, binary lung masks were provided for each scan pair. In the EMPIRE10 challenge, diffeomorphic demons was referenced as “Asclepios1”.

To register each pair of images, we first performed a global affine registration between the fixed and moving images using the method proposed by Ourselin et al. [?]. This registration method is based on a multi-scale block-matching algorithm, and, in its original version, this method allowed to estimate a rigid transformation between two images. Since the paper publication, the code has been adapted in order to estimate an affine transformation. In this paper, we used the affine version of this registration method. The parameters used for the challenge was:

- Number of pyramid level: 4
- Number of iteration at each level: 6
- Type of estimator: weighted least trimmed squares

The value of other parameters was set by default. This first linear registration allowed to compensate for the global deformation induced by change in position of the patient or by the lung position in the breathing cycle. To focus on the lung part, the affine registration was performed on the masked images. The resulting affine transformation was converted into a deformation field and then given as an initial field to the diffeomorphic demons.

The implementation of the diffeomorphic demons used for the challenge was based on ITK and was originally presented in [?]. This implementation is generic and consequently applies for chest CT registration as well as any image registration problems (brain, heart, etc.). The method used is fully automatic since the parameters were the same for any pair of images:

- No fluid-like smoothing was used
- Elastic-like smoothing: Gaussian kernel with $\sigma_T = 2.5$
- Number of pyramid level: 4
- Maximum step length: 2

Both registration processes have been performed on masked images and no histogram equalization has been applied on these images. The implementation of the diffeomorphic demons is available in the MedINRIA software platform³.

³ <http://www-sop.inria.fr/asclepios/software/MedINRIA/>

3.2 Numerical results

Table 1 presents the results of the EMPIRE10 challenge for the diffeomorphic demons algorithm. For each pair of images, the registration method was evaluated by four criteria:

- Alignment of lung boundaries
- Alignment of major fissures
- Correspondence of annotated point pairs
- Analysis of singularities in the deformation field

Thanks to the bijective nature of the diffeomorphisms, the diffeomorphic demons had a perfect score on singularities in the deformation field. The method also appeared to be very efficient on alignment of lung boundaries with an almost perfect score. The performance on alignment of major fissures and on annotated point correspondence were more than fair with a respective average rank of 15.97 and 13.67 (out of 34). Overall, our approach appeared to be a very efficient registration method for thoracic CT images with a rank of 9 among the 34 competing algorithms. In particular, it outperformed several state of the art methods highly specialized and optimized for thoracic CT images.

3.3 Visual results

In this section, we present some visual results illustrating the performance of our method. The presented images correspond to axial slices of the lungs. In order to focus the reader attention onto the lungs, the contrast in these regions has been artificially increased while the contrast outside has been decreased. This manipulation on the contrast was possible thanks to the masks provided for both fixed and moving images. Since the registered image is supposed to perfectly match the fixed image, the contrast change of the registered image has been performed using the mask of the fixed image. As a consequence, a misalignment of the lung boundary will appear as a thin white band in the lung mask and as a dark band outside of the mask.

According to Table 1, the registration process using the diffeomorphic demons was particularly accurate on the pairs of scans #9 and #15. Fig. 1 illustrates for both scan pairs, respectively from left to right, the moving source image, the registered source image, and the fixed target image. One can see that the initial data (fixed and moving images) are clearly not registered (lung boundaries, vessels, bronchus, etc.). Using our approach, the registered image appears to be very similar to the fixed image: the lung boundaries are correct and most of structures of the fixed image are present and well positioned in the registered image.

According to Table 1, our approach was less efficient on the scan pairs #14 and #20 (see Fig.2). Indeed, the lung boundary is not perfectly aligned and some structures (vessels and bronchus), visible in the fixed image, are not present in the registered image, and conversely. Moreover, one can see (especially on scan pair #20) that some vessels have been distorted due to the regularization

Scan Pair	Lung Boundaries		Fissures		Landmarks		Singularities	
	Score	Rank	Score	Rank	Score	Rank	Score	Rank
01	0.04	19.00	4.79	22.00	4.84	21.00	0.00	11.50
02	0.00	11.00	0.00	15.00	0.38	8.00	0.00	12.50
03	0.00	5.50	0.00	12.50	0.34	8.00	0.00	12.00
04	0.00	6.00	0.00	16.50	5.23	31.00	0.00	14.00
05	0.00	13.00	0.00	16.00	0.00	5.50	0.00	13.50
06	0.00	16.00	0.00	21.00	0.25	3.00	0.00	14.00
07	0.05	20.00	1.12	16.00	3.55	19.00	0.00	10.00
08	0.00	18.00	0.03	14.00	1.04	16.00	0.00	12.50
09	0.00	8.00	0.00	6.50	0.52	4.00	0.00	13.00
10	0.00	9.00	0.00	15.00	7.60	30.00	0.00	13.50
11	0.06	19.00	0.00	7.00	1.21	14.00	0.00	11.50
12	0.00	10.00	0.00	13.50	0.00	5.00	0.00	14.50
13	0.00	3.00	0.05	1.00	0.76	4.00	0.00	13.00
14	0.04	16.00	9.64	27.00	8.23	23.00	0.00	9.50
15	0.00	8.00	0.00	7.00	0.59	3.00	0.00	12.50
16	0.00	3.50	2.26	31.00	1.62	25.00	0.00	13.50
17	0.00	6.50	0.05	22.50	0.72	9.00	0.00	14.00
18	0.06	18.00	4.32	22.00	3.57	20.00	0.00	10.50
19	0.00	14.00	0.00	12.00	0.41	2.00	0.00	14.50
20	0.00	17.00	5.40	22.00	8.62	23.00	0.00	10.50
Avg	0.01	12.02	1.38	15.97	2.47	13.67	0.00	12.52
Average Ranking Overall								13.55
Final Placement								9

Table 1. Results for each scan pair, per category and overall. Rankings and final placement are from a total of 34 competing algorithms.

applied to the deformation field. However, even if not perfect in these cases, the two registered images are very similar to their corresponding fixed target images which shows the overall quality of the results.

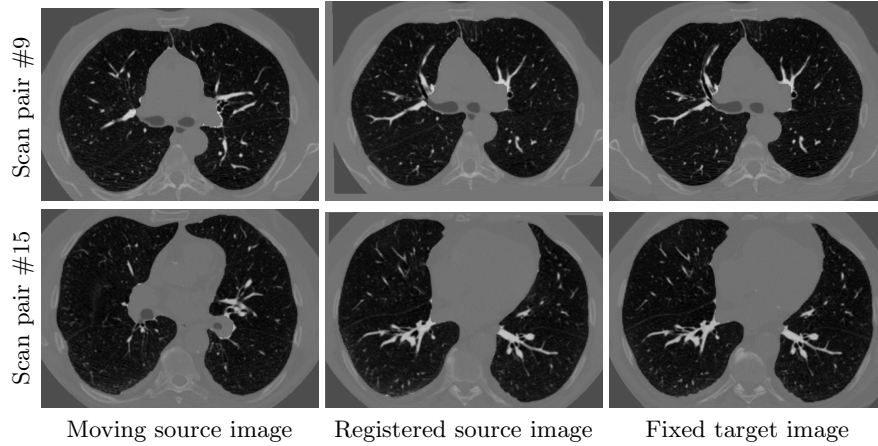


Fig. 1. Image registration results (two of the most accurate examples according to Table 1). The registered image (central column) is the moving image (left column) re-sampled in the geometry of the fixed image (right column). The slice numbers are 292 for the scan pair #9, and 157 for the scan pair #15.

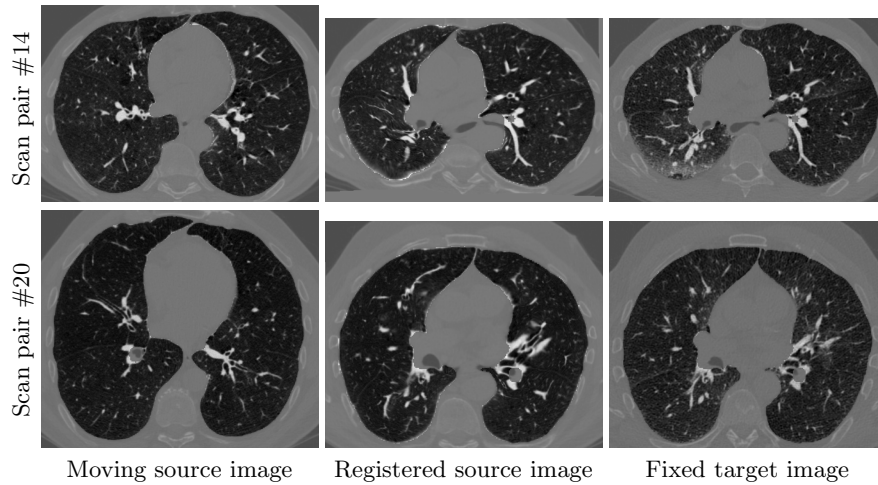


Fig. 2. Image registration results (two of the less accurate examples according to Table 1). The slice numbers are 226 for the scan pair #14, and 161 for the scan pair #20.